Fusion Engineering and Design 89 (2014) 1653–1657

Contents lists available at ScienceDirect

Fusion Engineering and Design

journal homepage: www.elsevier.com/locate/fusengdes

Compatibility of Ni and F82H with liquid Pb–Li under rotating flow

A. Kanai[a], C. Park[a], K. Noborio[a,b], R. Kasada[a,*], S. Konishi[a], T. Hirose[c], T. Nozawa[d], H. Tanigawa[d]

[a] Institute of Advanced Energy, Kyoto University, Gokasho, Uji, Kyoto 611-0011, Japan
[b] Hydrogen Isotope Research Center, University of Toyama, Toyama 930-8555, Japan
[c] Japan Atomic Energy Agency, 801-1 Mukoyama, Naka, Ibaraki 3110193, Japan
[d] Japan Atomic Energy Agency, Fusion Research and Development Directorate, Division of Rokassho BA Project, Structural Materials Development Group, 2-166 Omotedate, Obuchi, Rokkasho, Aomori 039-3212, Japan

GRAPHICAL ABSTRACT

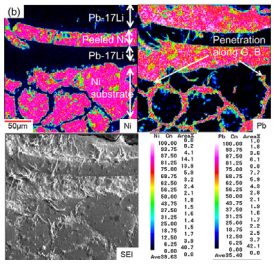

ARTICLE INFO

Article history:
Received 12 September 2013
Received in revised form 27 February 2014
Accepted 3 March 2014
Available online 25 March 2014

Keywords:
Liquid blanket
Structural material
Li–Pb
Reduced-activation ferritic steel
Liquid metal embrittlement

ABSTRACT

The present study reports the compatibility of a reduced-activation ferritic steel F82H and Ni with liquid Pb–Li under rotating flow conditions at 600 °C. Cross-sectional observation of Ni using field emission electron probe micro-analyzer (FE-EPMA) after exposure for 100 h revealed that severe grain boundary penetration of Pb into Ni occurred up to approximately a depth of 700 μm, causing liquid metal embrittlement (LME). In contrast, the results for F82H after exposure for 500 h showed the formation of pitting holes and a Cr-depleted layer at the surface with an approximate maximum depth of 10 μm. Oxide particles were also found in the Pb–Li region in the F82H specimen after exposure. The radio-frequency glow discharge spectrometers successfully detected Li and indicated Li oxide formation at the surface.

1. Introduction

Reduced-activation ferritic martensitic (RAFM) steels are candidate structural materials for blanket modules used in liquid metal coolants in a fusion reactor [1]. F82H, a Japanese RAFM steel, has attracted attention because of its excellent resistance against neutron irradiation below 550 °C [2]. Employing Pb–17Li as a coolant makes the blanket design simple as it works also as a tritium breeder. Such a combination of an RAFM steel and a liquid metal can be used as a test blanket module (TBM) in an International Thermonuclear Experimental Reactor (ITER) [3].

When materials are used in flowing coolants, they may suffer from corrosion, erosion and/or flow-accelerated corrosion (FAC). In the case of liquid metal coolants, furthermore, the liquid metal embrittlement (LME) due to a penetration of liquid metal into the material along their grain boundary is an important degradation issue [4]. Some of these phenomena are influenced by the relative velocity of the flowing liquid at the surface of the materials.

* Corresponding author. Tel.: +81 774 38 3431; fax: +81 774 38 3439.
E-mail address: r-kasada@iae.kyoto-u.ac.jp (R. Kasada).

http://dx.doi.org/10.1016/j.fusengdes.2014.03.008
0920-3796/

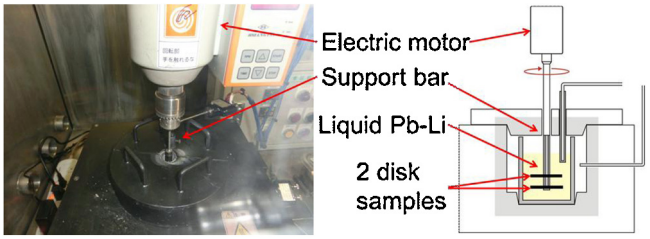

Fig. 1. Apparatus to rotate disk samples.

Therefore, evaluating the compatibility related to flow rates is important. There are not many reports of the compatibility of RAFMs with Pb–17Li under flowing conditions. The objective of this study is to investigate the compatibility of a RAFM with flowing liquid Pb–17Li using a rotating disk apparatus. Compared with the large loop technique, the rotating disk method has the advantage of being a more convenient way to investigate the effect of liquid metal flow on the compatibility of materials [5–8]. Experiments have also been conducted with a pure-Ni specimen, as Ni is known to be corroded easily by Pb and Pb–Li [9,10].

2. Experimental method

The materials used in this study were F82H-IEA (Fe-8Cr-2WVTa-0.1C) produced by JAEA and commercial pure Ni (99.99%). The specimens were cut into disks of 50 mm in diameter and 2 mm in thickness. These disks had a 5.5-mm-diameter hole to fix the support rod of the rotating apparatus mentioned below. Before testing, the specimens were polished mechanically to achieve a mirror finish; #4000 SiC paper was used to reduce the surface roughness.

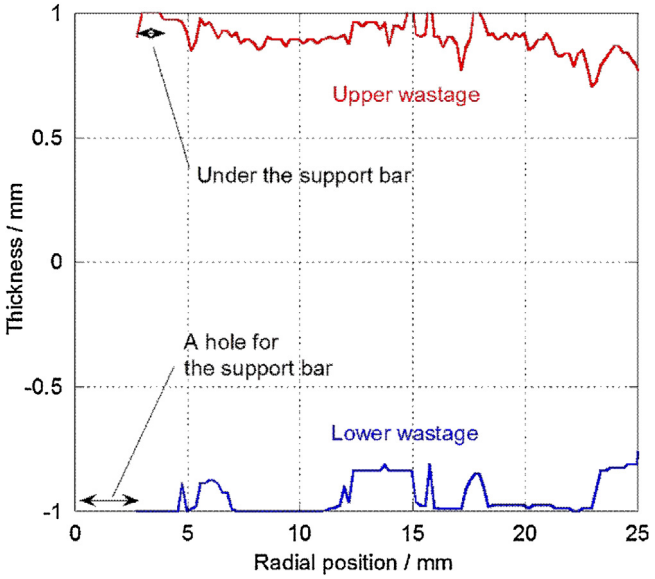

Fig. 3. Change of thickness and amount of corrosion of pure Ni after 100 h test in Pb–17Li.

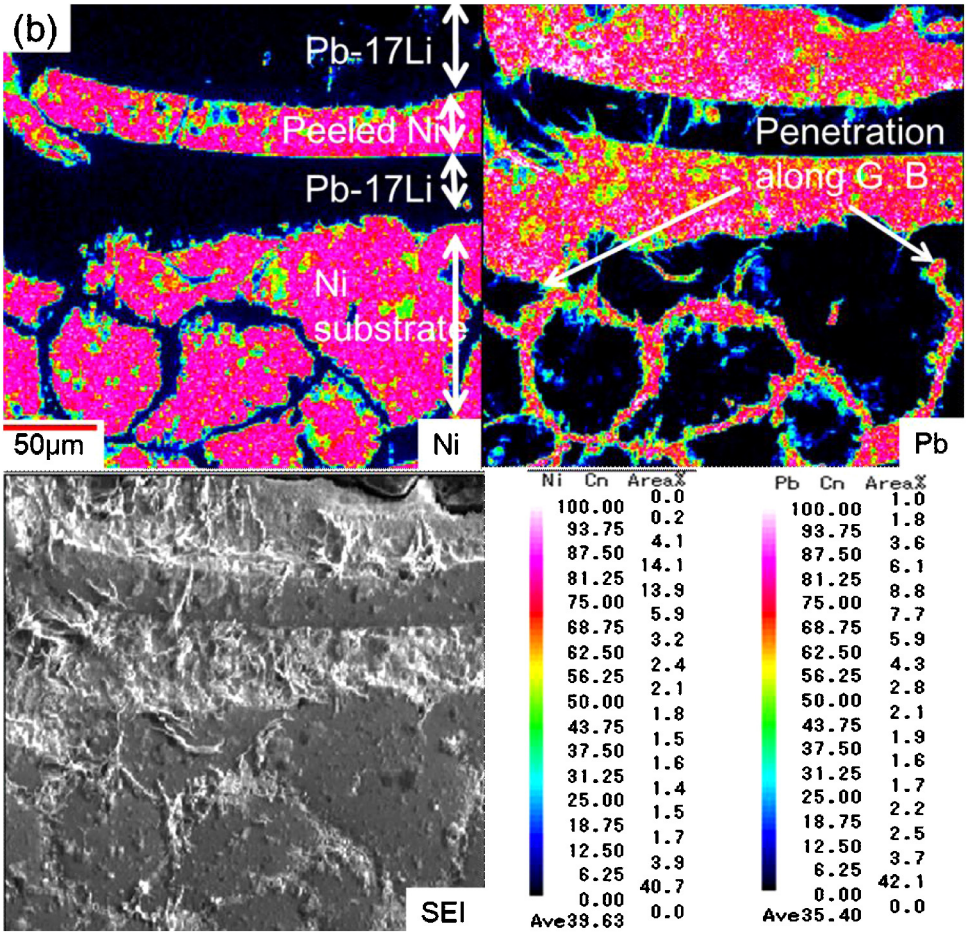

Fig. 2. Results of EPMA analysis on the cross-section of the whole pure-Ni specimen after 100 h test in Pb–17Li, (a) all the Ni and Pb, (b) scale-up interface and penetration part of Ni and Pb.

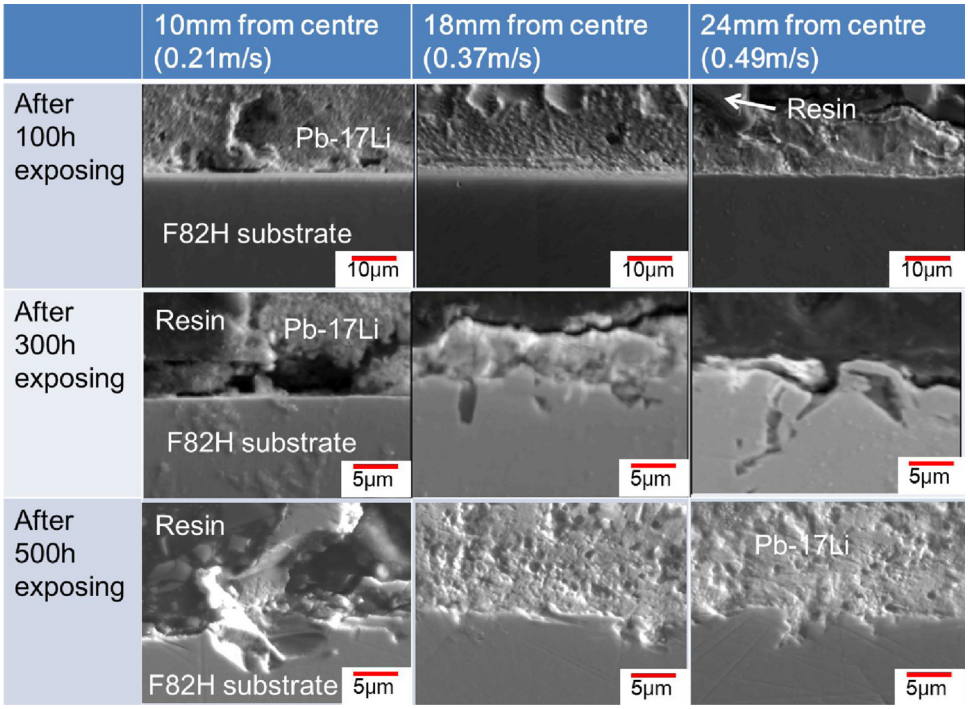

Fig. 4. SEM images of cross-section of F82H after 100 h and 300 h test in Pb–17Li.

The device to rotate disk materials in liquid Pb–Li is shown in Fig. 1. Two disk samples were mounted on the support rod at a distance of 2.75–3.75 mm. After mounting, both F82H and pure Ni were exposed to 1.5 kg of Pb–17Li. Testing duration of F82H was 100 h, 300 h, and 500 h, and that for pure Ni was 100 h. For both materials, temperature was kept at 600 °C for accelerated condition. Rotating speed was 200 rpm, which corresponds to a range of 0.15–0.52 m/s of circumferential velocity, a function of the radial position on the disk, for static Pb–17Li.

This rotating apparatus was placed in a glove box filled with high-purity argon gas, and the atmosphere was controlled at O_2 <0.1 ppm and moisture <0.1 ppm. All materials for the crucible and support rod were made from molybdenum, which was expected to be compatible with the Pb–Li alloy [5,12–14].

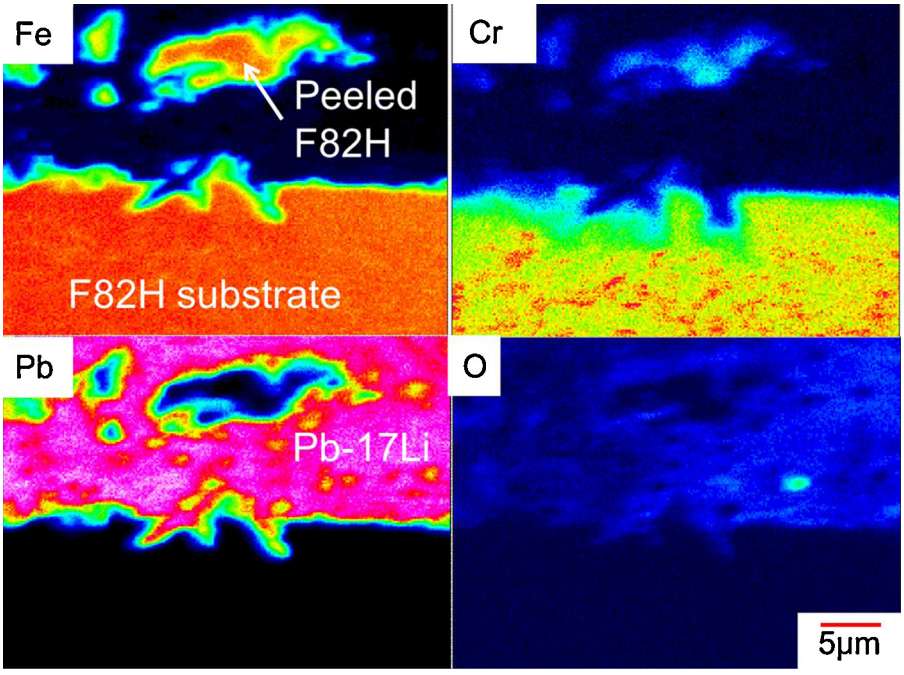

Fig. 5. Results of EPMA analysis on the cross-section of F82H after 500 h test in Pb–17Li. Cr-depleted zone was observed.

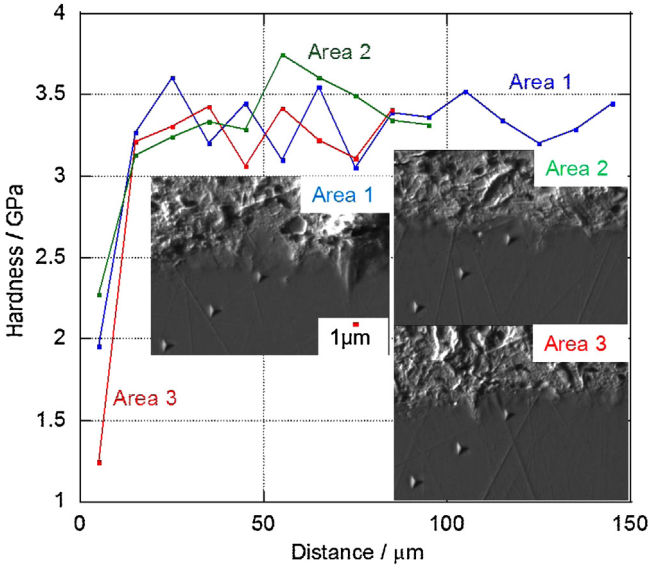

Fig. 6. Hardness at different distances from the interface between solid Pb–17Li and F82H after 500 h test in Pb–17Li.

After the Pb–17Li corrosion experiments, microstructural observation, and elemental mapping analysis were carried out using JEOL JXA-8530F field emission electron micro-prove analyzer (FE-EPMA). The radio-frequency glow discharge spectrometers (rf-GD-OES) and a Horiba GD-Profiler 2 were used to evaluate the depth profiles of Li, Pb, Fe, Cr, and W on the 2 mm diameter area in the corroded specimen. In particular, rf-GD-OES was used to measure the depth-profile of Li since it cannot be detected by conventional X-ray spectrometers [11]. Nano-indentation hardness test was carried out using an Elionix ENT-1100a with a maximum depth of 300 nm.

3. Result and discussion

3.1. Compatibility of pure Ni with Pb–17Li

The elemental maps of Ni and Pb at a cross-section of the rotating disk for the pure-Ni specimen after testing at 600 °C for 100 h at 200 rpm were obtained by FE-EPMA as shown in Fig. 2. An intergranular penetration of Pb into the Ni substrate was found to occur to an approximate depth of 700 μm from the final surface of the Ni substrate when the surface was inhomogeneously eroded. This kind of rapid penetration of a liquid metal into Ni along the grain boundaries was previously reported for Ni in static liquid Bi at 700 °C for 16 h, resulting in a strong brittleness due to the intergranular cracking [9]. Such a LME was observed as a result of the peeling off of Ni grain at the surface region of the corroded specimen as shown in Fig. 2(b). Fig. 3 presents the thickness change of a pure-Ni specimen for different radial positions r from the center of the sample. The thickness data was calculated from the cross-sectional map of Ni in Fig. 2(a). No data at r = 0–2.75 mm corresponds to the center hole of the specimen. The region of r = 2.75–3.75 mm possessed a surface line as this part was covered by the support rod except for the chipped edge point. The thickness reduction increased with r, thus corresponding to the higher circumferential velocity. However, local thickness reductions were observed especially on the bottom side. As shown in Fig. 1, the underside of the specimen faced the shallow channel of the Pb–Li flow, in contrast to the upper side. It is assumed that a combination of LME at the grain boundaries due to the existence of Pb and the rotating flow condition causes the erosion and corrosion in the pure Ni. Further analysis on the flowing condition in the rotating disk apparatus is needed.

3.2. Compatibility of F82H with Pb–17Li

Fig. 4 shows cross-sectional SEM images of F82H after 100 h, 300 h, and 500 h tests in Pb–17Li. Although the Pb–17Li effect was not so severe as compared to the case with pure Ni, some pitting holes with a depth of 18 μm were observed at the surface and more

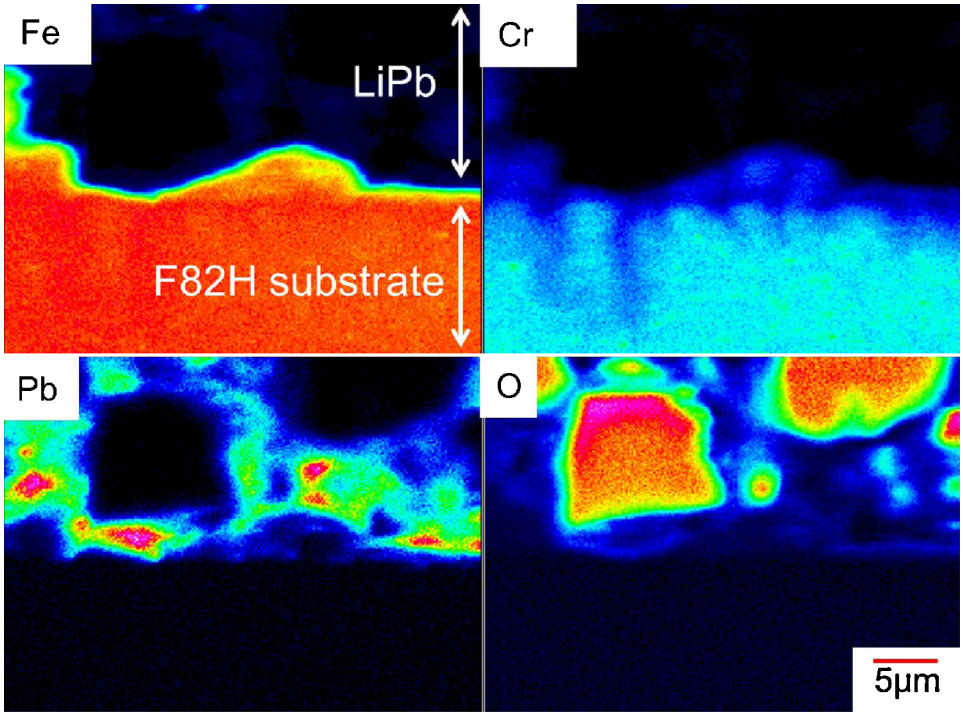

Fig. 7. Results of EPMA analysis on the cross-section of F82H after 500 h test in Pb–17Li. Oxides on the specimen surface were observed.

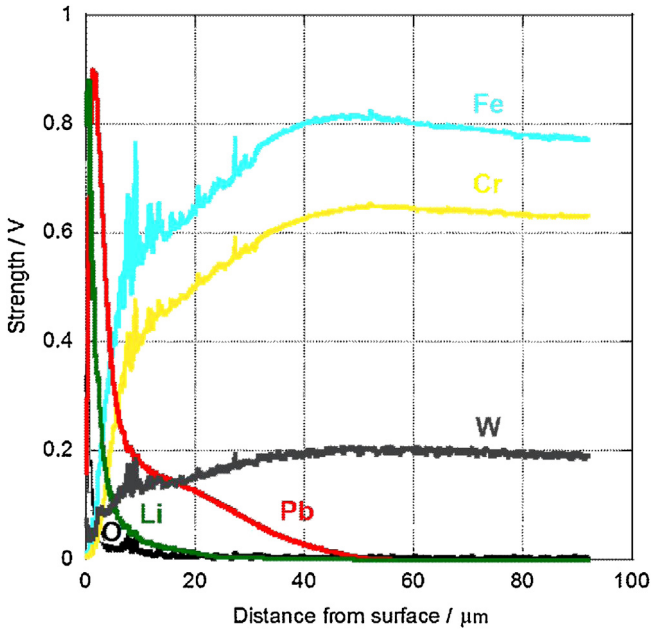

Fig. 8. Depth-profile of elements of F82H after 300 h test in Pb–17Li obtained by rf-GD-OES.

away from the center when in contact with Pb–17Li for 300 h. In contrast, any surface of F82H after 100 h exposure was uniformly flat as in its initial state. The pitting holes were observed at all positions after 500 h. This result means that the surface morphology of F82H in Pb–17Li at 600 °C is strongly affected by the testing duration and flowing condition. The maximum depth of the pitting hole formed after testing for 300 h and 500 h was approximately 10 μm. Fig. 5 shows elemental maps from the same area as the SEM image (Fig. 4) of the sample after the 500 h test and at a distance of 24 mm from the center. It is found that Pb exists in the pitting holes and Cr-depleted layer over the whole surface region. In addition, Cr-rich phases were observed in the substrate region, where $M_{23}C_6$ probably disappears into the Cr-depleted layer. It is known that Cr has a relatively higher dissolution rate than Fe [15]. As shown in Fig. 6, nanoindentation hardness data near the interface between Pb–17Li and F82H after 500 h test in Pb–17Li shows softening by 1–2 GPa of the F82H to 5 μm depth from the interface which corresponds to the Cr-depleted layer. Such softening in the surface of F82H probably affects the erosion resistance. Kondo et al. showed a penetration of Pb along the grain boundary and lath boundary in JLF-1 RAFM steel at 600 °C [7,8]. Further work is underway to obtain data for F82H at longer duration times.

The state of Li in the corroded Ni and F82H is still unclear as it is not possible for wavelength-dispersed X-ray spectrometers in FE-EPMA to detect the Li directly because of their low X-ray energy and emission. As shown in Fig. 7, at 23 mm away from the center, some of the oxides on the specimen surface do not include Pb and other detectable elements. In order to investigate the state of the oxide at the surface of the specimen, rf-GD-OES was employed to examine the surface of F82H after the 300 h test in Pb–17Li. Fig. 8 displays the depth-profile of the elements such as Fe, Cr, W, O, Li and Pb obtained by rf-GD-OES. Solid Pb–17Li remained partially on the surface, while the existence of both Pb and Li was confirmed. However, Li was only observed at a shallow depth area containing O of ~25 μm, while Pb was found to exist at depths above 40 μm. These results indicate that Li-oxide is formed on the surface of the specimens, which may have an important role in determining compatibility.

4. Conclusion

We investigated the compatibility of pure Ni and F82H RAFM steel with Pb–17Li under rotating flow conditions. The results obtained are as follows:

1) When pure Ni is exposed to liquid Pb–17Li under rotating flow conditions at 600 °C, significant grain boundary penetration and peeling-off of grain occurs. As a result, the thickness of the specimen decreased.
2) The F82H RAFM steel shows good compatibility, as evaluated on the basis of the specimen's surface morphology after a 100 h test in liquid Pb–17Li under rotating flow conditions at 600 °C. However, the specimen exhibits local pitting corrosion and a Cr-depleted layer at the surface with an approximate maximum depth of 10 μm after 500 h.
3) The existence of Li at the surface region of F82H after exposure was confirmed by rf-GD-OES, indicating Li oxide formation.

Acknowledgments

The authors thank Dr. Masaru Nakamichi for his help with the FE-EPMA. The authors acknowledge Mr. Fumito Okino for his valuable comments. This research was partially supported by the Japan Atomic Energy Agency under the Joint Work Contract 24k572.

References

[1] C.P.C. Wong, J.-F. Salavy, Y. Kim, I. Kirillov, E.R. Kumar, N.B. Morley, et al., Fusion Eng. Des. 83 (2008) 850–857.
[2] H. Tanigawa, T. Hirose, K. Shiba, R. Kasada, E. Wakai, H. Serizawa, et al., Fusion Eng. Des. 83 (2008) 1471–1476.
[3] J.-F. Salavy, G. Aiello, P. Aubert, L.V. Boccaccini, M. Daichendt, G. De Dinechin, et al., J. Nucl. Mater. 386–388 (2009) 922–926.
[4] M.G. Nicholas, C.F. Old, J. Mater. Sci. 14 (1979) 1–18.
[5] C. Park, K. Noborio, Y. Yamamoto, S. Konishi, J. Nucl. Mater. 417 (2011) 1218–1220.
[6] Ph. Deloffre, A. Terlain, A. Alemany, A. Kharicha, Fusion Eng. Des. 69 (2003) 391–395.
[7] M. Kondo, T. Muroga, A. Sagara, T. Valentyn, A. Suzuki, T. Terai, et al., Fusion Eng. Des. 86 (2011) 2500–2503.
[8] M. Kondo, M. Takahashi, T. Tanaka, T. Valentyn, T. Muroga, Fusion Eng. Des. 87 (2012) 1777–1787.
[9] M.G. Barker, T. Sample, The solubilities of nickel, manganese and chromium in Pb–17Li, Fusion Eng. Des. 14 (1991) 219–226.
[10] K. Shiba, A. Hishinuma, A. Tohyama, K. Masamura, JAERI-Tech 97-038, 1997.
[11] W. Luesaiwong, R.K. Marcus, Microchem. J. 74 (2003) 59–73.
[12] F. Barbier, P. Deloffire, A. Terlain, J. Nucl. Mater. 307 (2002) 1351–1354.
[13] B. Pint, J. Moser, P. Tortorelli, Fusion Eng. Des. 81 (2006) 901–908.
[14] B. Pint, J. Moser, P. Tortorelli, J. Nucl. Mater. 367–370 (2007) 1150–1154.
[15] H.U. Borgstedt, H. Feuerstein, J. Nucl. Mater. 191–194 (1992) 988–991.